Use of a 3D Virtually Reconstructed Patient-Specific Model to Examine the Effect of Acetabular Labral Interference on Hip Range of Motion

Shota Higashihira,*† MD, PhD, Naomi Kobayashi,*‡ MD, PhD, Hyonmin Choe,† MD, PhD, Kosuke Sumi,† and Yutaka Inaba,† MD, PhD

Investigation performed at the Department of Orthopaedic Surgery, Yokohama City University, Yokohama, Japan

Background: The labrum is likely to influence impingement, which may also depend on acetabular coverage. Simulating impingement using 3-dimensional (3D) computed tomography (CT) is a potential solution to evaluating range of motion (ROM); however, it is based on bony structures rather than on soft tissue.

Purpose: To examine ROM when the labrum is considered in a 3D dynamic simulation. A particular focus was evaluation of maximum flexion and internal rotation angles before occurrence of impingement, comparing them in cases of cam-type femoroacetabular impingement (FAI) and borderline developmental dysplasia of the hip (BDDH).

Study Design: Descriptive laboratory study.

Methods: Magnetic resonance imaging (MRI) and CT scans of 40 hips (20 with cam-type FAI and 20 with BDDH) were reviewed retrospectively. The thickness and width of the labrum were measured on MRI scans. A virtual labrum was reconstructed based on patient-specific sizes measured on MRI scans. The impingement point was identified using 3D dynamic simulation and was compared with the internal rotation angle before and after labral reconstruction.

Results: The thickness and width of the labrum were significantly larger in BDDH than in FAI ($P < .001$). In FAI, the maximum internal rotation angles without the labrum were 30.3° at 90° of flexion and 56.9° at 45° of flexion, with these values decreasing to 18.7° and 41.4°, respectively, after labral reconstruction ($P < .001$). In BDDH, the maximum internal rotation angles were 48.0° at 90° of flexion and 76.7° at 45° of flexion without the labrum, decreasing to 31.1° and 55.3°, respectively, after labral reconstruction ($P < .001$). The differences in the angles before and after labral reconstruction were larger in BDDH than in FAI (90° of flexion, $P = .03$; 45° of flexion, $P = .01$).

Conclusion: As the labrum was significantly more hypertrophic in BDDH than in FAI, the virtual labral model revealed that the labrum's interference with the maximum internal rotation angle was also significantly larger in BDDH.

Clinical Relevance: The labrum has a significant effect on impingement; this is more significant for BDDH than for FAI.

Keywords: acetabular labrum; femoroacetabular impingement; borderline developmental dysplasia of the hip; computer simulation

Hip arthroscopic surgery and related diagnostic techniques for femoroacetabular impingement (FAI) and borderline developmental dysplasia of the hip (BDDH) with labral tear have progressed over the past decade. FAI is a fundamental pathophysiology caused by impingement between the acetabulum and the bony prominence of the femoral head-neck junction, that is, cam morphology.[9] This kind of impingement is often accompanied by labral tear.[2] Pierannunzii[22] reported that cam-type FAI is based on shear stress and that pincer-type FAI determines contact stress between the acetabulum and the femoral neck, thereby squeezing the labrum. By contrast, the main pathological condition in developmental dysplasia of the hip (DDH) is hip joint instability due to a shallow and dysplastic bony acetabular roof.[7,8] Dysplasia increases the load on the hip by 2.8 to 4.0 times[12]; therefore, the load stress might be the main cause of labral damage in cases of dysplasia. In addition, the coexistence of DDH and cam deformity has been recognized,[14] and such overlapping pathology must be noted. Both load stress on the hip and dynamic stress due to cam deformity may coexist in BDDH cases. Thus, in

The Orthopaedic Journal of Sports Medicine, 8(11), 2325967120964465
DOI: 10.1177/2325967120964465

BDDH, several factors (eg, joint instability, labral tear, and impingement) caused by cam deformity may interact.

Previous studies have used 3-dimensional (3D) dynamic simulations based on preoperative computed tomography (CT) images to evaluate the impingement point before surgery.[15,16] While such 3D dynamic simulations have important clinical implications with respect to identifying the bony impingement point, they do not take into account the effect of soft tissue, including the labrum. Although magnetic resonance imaging (MRI) is one of the most reliable modalities for evaluating soft tissue around the hip joint,[1,24] only a few studies have reported the use of MRI for dynamic analysis, and these were related to the shoulder joint.[11,21] Although the mechanical forces in FAI and BDDH are quite different, the labrum is damaged in both of these conditions. Thus, the clinical question is to what extent the acetabular labrum interferes with movement of the hip joint before it becomes impinged between the acetabular rim and femoral neck. Previous studies using computer simulation analysis were unable to consider the effect of the labrum.

The utility of radial sequence 3-T 3D multiple echo recombined gradient echo (MERGE) MRI for evaluating the labrum before arthroscopic surgery has previously been confirmed, with good definition of the labral shape being demonstrated.[13] 3D MERGE MRI can be used not only to diagnose a labral tear, but also to clearly define the size of the labrum. In this study, we hypothesized that a virtual labrum could be reconstructed in a bone model specific to each patient, using one's specific labral size identified on 3D MERGE MRI scans. Thus, a virtual labral model was reconstructed using patient-specific data combined with a CT bone model created using Zed Hip software (LEXI Co Ltd).

The purpose of this study was to examine the range of motion (ROM) in 3D dynamic simulations that take the labrum into consideration. In particular, we evaluated the maximum flexion and internal rotation angles at which impingement occurred, making comparisons between FAI and BDDH. The hypothesis of this study was that the acetabular labrum influences the impingement condition before bony impingement occurs.

METHODS

This study was approved by the institutional review board of Yokohama City University. We retrospectively reviewed 3D MERGE MRI scans and CT images acquired for preoperative evaluation before hip arthroscopic surgery; the images were acquired between April 2014 and September 2018. Of 91 consecutive hips, 42 were excluded because of the following: 7 did not have available MERGE MRI or CT data, 10 had a history of surgery on the same joint (total hip arthroplasty, osteotomy, or primary arthroscopic surgery), and 25 did not match any of the diagnostic criteria for FAI or BDDH on radiographs (ie, synovial osteochondromatosis, labral tear after trauma, osteonecrosis, or osteoarthritis). The remaining 49 hips included 26 with cam-type FAI, 3 with combined-type FAI, and 20 with BDDH (10 BDDH with cam-type FAI and 10 BDDH without cam-type FAI). To allow evaluation of the same number of hips for each disease, the most recent 20 consecutive joints with cam-type FAI were included in the study. Thus, a total of 40 joints (20 with cam-type FAI and 20 with BDDH) were analyzed. The patients and their characteristics were assessed by a single responsible surgeon (N.K.). The mean ages at the time of surgery were 37 years (range, 14-58 years) in the cam-type FAI group and 42 years (range, 15-63 years) in the BDDH group. The cam-type FAI cases included 12 male and 5 female patients, and the BDDH cases included 4 male and 14 female patients. In all cases, 3D MERGE MRI and CT analyses were performed within the 4 months before surgery.

Radiographic Evaluation

The following radiographic definitions of FAI and BDDH were used: cam-type FAI was defined as an alpha angle $>55^\circ$ on the cross-table lateral view or 45° on the flexion Dunn view[5,27]; pincer-type FAI was defined as a center-edge (CE) angle $>40^\circ$ on the anteroposterior view of the pelvis.[18] Combined-type FAI was defined as the presence of both cam and pincer deformities. BDDH was defined as a CE angle between 20° and 25° on the anteroposterior view of the pelvis.[3] Yamasaki et al[27] reported that a CE angle $>25^\circ$ should be excluded from the FAI criteria, even if there were findings consistent with FAI. Therefore, patients with a CE angle of 20° to 25° were classified as having BDDH with cam deformity (alpha angle $>55^\circ$).

MERGE MRI Findings

All MRI evaluations were performed using 3D MERGE MRI acquired on a 3-T Discovery MR750w scanner (GE Healthcare Co Ltd). Axial sequences were obtained with a repetition time of 30 milliseconds, an average echo time of 10.9 milliseconds, a field of view of 300×300 mm, a matrix of 300×300, a bandwidth of 50 kHz, a slice thickness of 1 mm, a section gap of 0 mm, and an acquisition time of 5 minutes. The average duration between MRI and surgery was 58 days (range, 5-102 days).

‡Address correspondence to Naomi Kobayashi, MD, PhD, Department of Orthopaedic Surgery, Yokohama City University Medical Center, 4-57 Urafune-cho, Minami-ku, Yokohama 232-0024, Japan (email: naomik58@aol.com).

*Department of Orthopaedic Surgery, Yokohama City University Medical Center, Yokohama, Japan.

†Department of Orthopaedic Surgery, Yokohama City University, Yokohama, Japan.

Final revision submitted May 1, 2020; accepted June 8, 2020.

The authors declared that there are no conflicts of interest in the authorship and publication of this contribution. AOSSM checks author disclosures against the Open Payments Database (OPD). AOSSM has not conducted an independent investigation on the OPD and disclaims any liability or responsibility relating thereto.

Ethical approval for this study was obtained from Yokohama City University Medical Center.

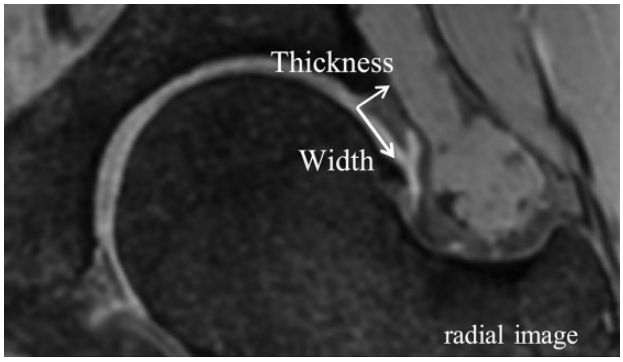

Figure 1. Labral thickness and width on multiple echo recombined gradient echo magnetic resonance imaging scan of a left-side hip joint. We measured the thickness of the acetabular labrum at the rim and the width to the apex of the acetabular labrum in the anterior region (2-3 o'clock), anterolateral region (1-2 o'clock), and lateral region (12-1 o'clock).

Radially reconstructed images were obtained using a multiplanar reconstruction procedure that reconstructed the axial images into the radial plane. The radial plane was obtained with a field of view of 150 × 150 mm and a slice thickness of 2 mm. Images were reconstructed every 5° around the center of the femoral neck axis defined on the axial and sagittal planes. Radial images were evaluated according to a clockface description, with 0° (3 o'clock) being anterior and 90° (12 o'clock) being lateral. On 3D MERGE MRI, the labrum was evaluated using radial imaging in the anterior region (2-3 o'clock), anterolateral region (1-2 o'clock), and lateral region (12-1 o'clock). Specifically, the thickness of the labrum at the acetabular rim and the width to the apex of the labrum were measured in each region (Figure 1).

The average thickness and width were calculated in each case. All MRI measurements were evaluated by an orthopaedic surgeon (S.H.) and a medical research student (K.S.) who were blinded to all other information. Intraobserver and interobserver reliability were calculated for all measurements of labral size.

CT Imaging Conditions

The average duration between CT and surgery was 64 days (range, 12-118 days). Each patient underwent CT examination of the pelvis and both femurs in the supine position. The CT images were acquired on a Sensation 16 (Siemens AG) using a tube voltage of 140 kV, current of 300 mA, and slice thickness of 1.5 mm.

3D Dynamic Simulation

A virtual acetabular labral model was reconstructed using Zed Hip software, based on the specific size of each individual labrum on 3D MERGE MRI scans. 3D bone models of the pelvis and both femurs were reconstructed using Zed Hip applied to the CT data. In this study, the functional pelvic plane in the supine position was used as the baseline for the pelvic plane. For the femoral plane reference, reference points around the femoral head on the axial and sagittal planes were used to define the femoral head center. Points on the medial/lateral epicondyles and posterior condyles, knee center, greater trochanter tip, and lesser trochanter were also identified.

Next, Zed Hip was used to reconstruct a virtual labral model based on the data measured on each horizontal slice of 3D MERGE MRI scans. Specifically, the labrum was considered to be represented as a triangle (with the average thickness of the labrum forming the base and the distance to the apex forming the height) on each horizontal slice (Figure 2).

The impingement point was identified using a 3D dynamic simulation created using Zed Hip. The impingement points on the femoral head-neck junction at 45° and 90° of flexion at the maximum internal rotation angle of the hip joint were evaluated. Bony impingement referred to contact between the acetabular rim and the femoral head-neck junction (Figure 3).

In the impingement simulation, the labral interference was defined as that between the virtual labrum and the femoral head-neck junction (Figure 4).

The maximum internal rotation angles before and after labral reconstruction were compared for each disorder. If the impingement point appeared at <45° or <90° of flexion, the patient was excluded.

Statistical Analysis

Statistical analyses were performed using R version 3.0.2 software (R Foundation for Statistical Computing). A P value <.05 was deemed significant. Differences in the measured size of the labrum among the 3 regions (anterior, anterolateral, and lateral) on 3D MERGE MRI scans were analyzed using 1-way analysis of variance, and differences between FAI and BDDH were evaluated using a t test. Differences between the maximum internal rotation angle before and after labral reconstruction were evaluated using the Wilcoxon signed rank test. The difference in angle between FAI and BDDH was evaluated using the Mann-Whitney U test. The 3D MERGE MRI findings were evaluated independently by 2 observers (S.H., K.S.), and the interobserver error was calculated by comparing the first and second evaluations made by a single observer. Intraclass correlation coefficients (ICCs) with 95% CIs were calculated for the interobserver and intraobserver agreement (moderate agreement, 0.5-0.75; good agreement, 0.75-0.9; excellent agreement, >0.9).[17]

RESULTS

Table 1 shows the results for the thickness of the labrum at the acetabular rim and the width to the apex of the labrum in each region, as measured on 3D MERGE MRI scans. The average thicknesses of the labrum at the acetabular rim were 4.54 mm in FAI and 5.97 mm in BDDH, with the labrum being significantly thicker in BDDH ($P < .001$). The

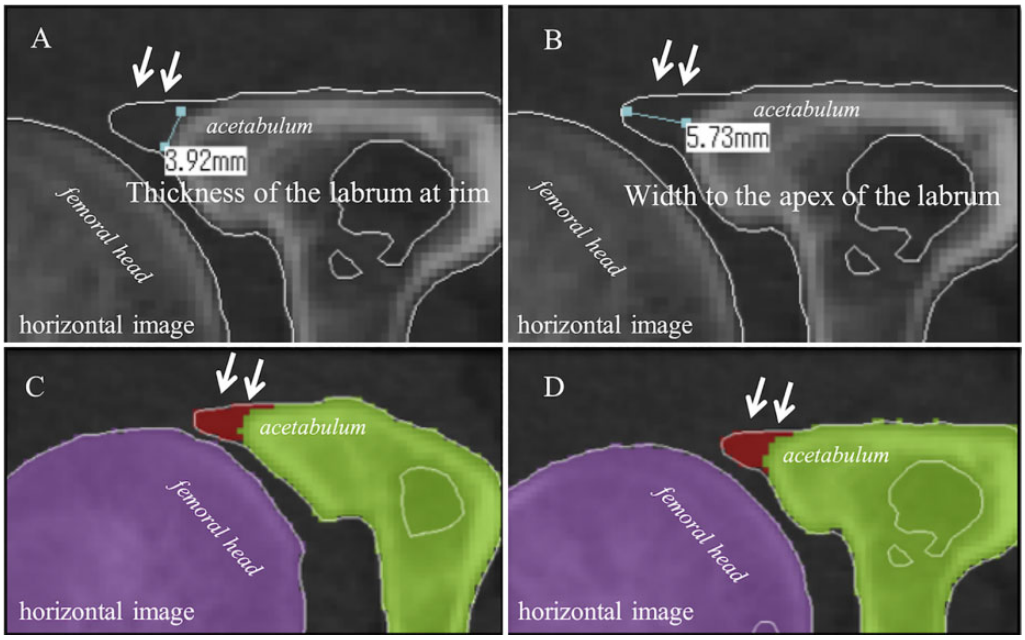

Figure 2. Reconstruction of the virtual acetabular labrum using Zed Hip (LEXI Co Ltd). Reconstruction of the acetabular labrum was based on its size measured on magnetic resonance imaging scans. The labral size was reflected in the Zed Hip reconstruction in each case. Specifically, the labrum was considered to be represented as a triangle on each horizontal slice, with the average thickness of the labrum forming the base and the distance to the apex forming the height (arrow in panels A and B, right-side hip joint). In this manner, the virtual labrum was added onto each slice using Zed Hip (arrow in panels C and D, right-side hip joint).

Figure 3. Simulation of bony impingement between the acetabulum and the femoral head-neck junction. The impingement point, identified using the Zed Hip (LEXI Co Ltd) 3-dimensional dynamic simulation, is shown by the arrow. The impingement points at (A) 90° (right-side hip joint) and (B) 45° (right-side hip joint) of flexion at the maximum internal rotation angle of the hip joint were evaluated.

average widths to the apex were 7.05 mm in FAI and 10.50 mm in BDDH, with this width being significantly higher in BDDH ($P < .001$).

The ICC for interobserver agreement for measurements made on 3D MERGE MRI scans was excellent ($\kappa = 0.93$), as was the intraobserver agreement ($\kappa = 0.97$). Figures 5 and 6 show the results for the maximum internal rotation angle before and after labral reconstruction in the 3D dynamic simulation using Zed Hip.

In FAI, the maximum flexion angle without the labrum was 103.9°. The maximum internal rotation angles were 30.3° (90° of flexion) and 56.9° (45° of flexion) at each flexion angle without the acetabular labrum. In BDDH, the maximum flexion angle was 120.0°. The maximum

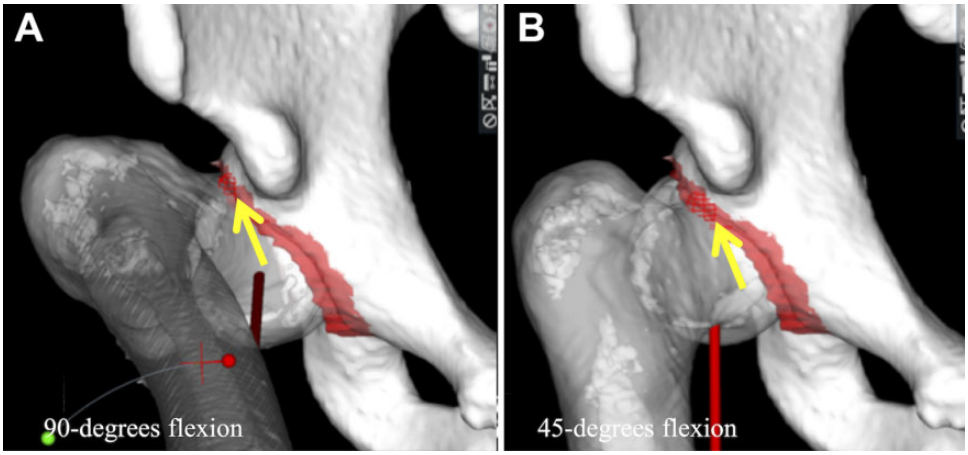

Figure 4. Simulation of the labral interference between the virtual acetabular labrum and the femoral head-neck junction. The virtual acetabular labrum on the acetabular rim is shown in red. The impingement point, identified using the 3-dimensional Zed Hip (LEXI Co Ltd) dynamic simulation, is shown by the arrow. The impingement points at (A) 90° (right-side hip joint) and (B) 45° (right-side hip joint) of flexion, with the maximum internal rotation angle, were evaluated.

TABLE 1
Average Thickness and Width of the Labrum in Each Region[a]

	Anterior		Anterolateral		Lateral		Total	
	Thickness[b]	Width[c]	Thickness	Width	Thickness	Width	Thickness	Width
FAI	3.76 ± 0.84	6.97 ± 2.07	5.00 ± 1.04	6.65 ± 2.08	4.86 ± 1.44	7.53 ± 1.69	4.54 ± 1.25	7.05 ± 1.96
BDDH	4.95 ± 1.47	11.12 ± 3.04	6.76 ± 1.70	9.93 ± 2.40	6.21 ± 1.67	10.47 ± 2.11	5.97 ± 1.76	10.50 ± 2.55
P value	.003	<.001	<.001	<.001	.009	<.001	<.001	<.001

[a]Data are reported in millimeters as mean ± SD. BDDH, borderline developmental dysplasia of the hip; FAI, femoroacetabular impingement.
[b]Thickness of the labrum at the acetabular rim.
[c]Width to the apex of the labrum from the acetabular rim.

internal rotation angles were 48.0° (90° of flexion) and 76.7° (45° of flexion) at each flexion angle without the acetabular labrum. After labral reconstruction, the maximum flexion angle in the simulation reflecting the measured size of the labrum on 3D MERGE MRI scans was 89.4°, and the maximum internal rotation angles were 18.7° (90° of flexion) and 41.4° (45° of flexion) in FAI. In BDDH, the maximum flexion angle was 103.6° and the maximum internal rotation angles were 31.1° (90° of flexion) and 55.3° (45° of flexion). In both diseases, there was a significant difference in the maximum flexion and internal rotation angles before and after labral reconstruction ($P < .001$).

The differences between the bony (without the acetabular labrum) impingement and the labral interference angle with the maximum internal rotation angle at 90° of flexion were 11.5° for FAI and 16.9° for BDDH (Figure 7).

The difference between the bony and labral interference angle was significantly larger in BDDH than in FAI ($P = .03$). Similarly, the difference between the bony and labral interference angle at the maximum internal rotation angle of 45° of flexion was significantly larger in BDDH (21.4°) than in FAI (15.5°; $P = .01$).

DISCUSSION

The most important clinical implication of this study is that the acetabular labrum has a significant effect on impingement in both FAI and BDDH. This effect is more significant for BDDH than for FAI. Hence, ROM based on computer simulation using a 3D bone model may be overestimated, particularly in cases of BDDH. In other words, the labrum interferes with the femoral head-neck junction before the ROM estimated by the bony impingement simulation. This has important clinical relevance when surgical treatment based on impingement simulation is being considered.

The results presented herein show that the acetabular labrum was significantly thicker and longer in cases of BDDH than in cases of FAI. This is compatible with a report by Garabekyan et al,[10] who showed that labral values at all locations were longer in cases of DDH and BDDH. The authors used MRI to measure the size of the labrum, showing normal acetabular coverage, acetabular overcoverage (>39°), BDDH (20°–24.9°), and DDH (<20°) at 3 locations (lateral, anterior, and anteroinferior). The results showed that the mean length of the labrum in DDH was statistically similar to that in BDDH. Multivariate

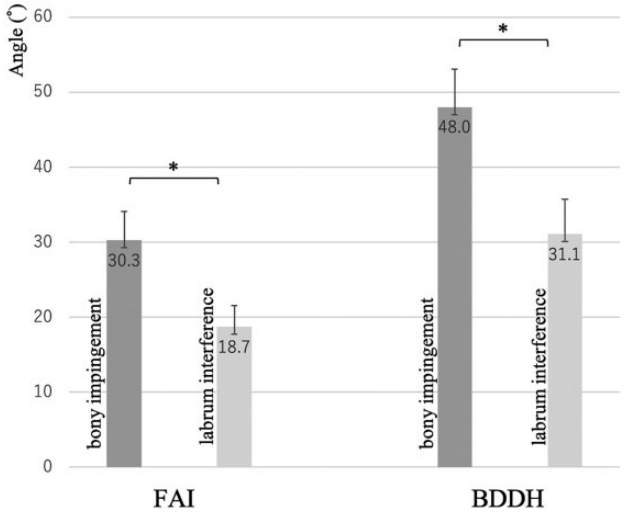

Figure 5. Difference in the maximum internal rotation angle at 90° of flexion in cases of bony impingement and labral interference. The maximum internal rotational angle was significantly lower in cases of labral interference (*$P < .001$). Error bars indicate SDs. BDDH, borderline developmental dysplasia of the hip; FAI, femoroacetabular impingement.

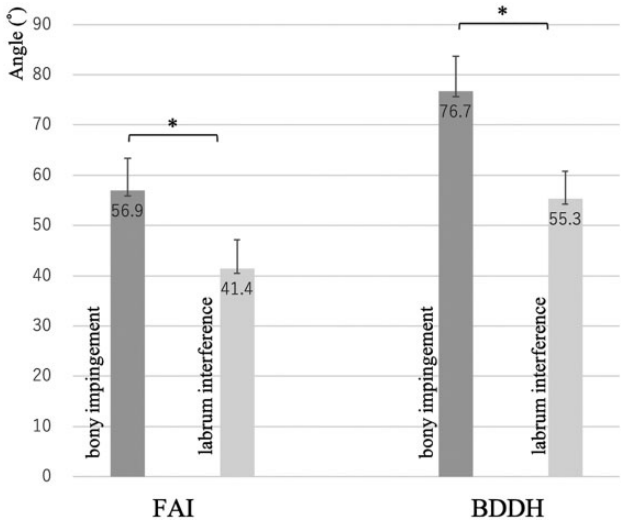

Figure 6. Differences in the maximum internal rotation angle at 45° of flexion between cases of bony impingement and cases of labral interference. The maximum internal rotational angle was significantly lower in cases of labral interference (*$P < .001$). Error bars indicate SDs. BDDH, borderline developmental dysplasia of the hip; FAI, femoroacetabular impingement.

analyses confirmed that the lateral CE angle was the strongest predictor of labral length, irrespective of measurement location. Lewis and Sahrmann[19] reported that the acetabular labrum is an important intra-articular structure of the hip joint, the labrum contributes the hip joint stability.

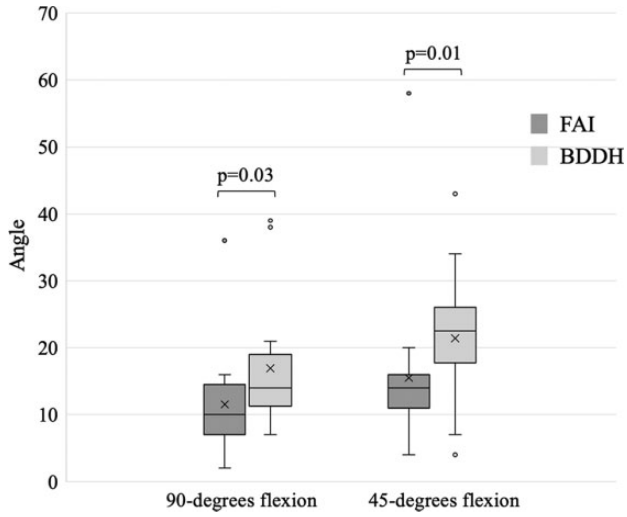

Figure 7. Differences between bony impingement and labral interference. The discrepancy (Δ angle) was significantly larger in cases of borderline developmental dysplasia of the hip (BDDH). Each box denotes the interquartile range. The line in the box represents the median value, and the cross denotes the average value. The error bar represents the maximum and minimum values. Dots represent outliers. FAI, femoroacetabular impingement.

They also reported that a labrum with insufficient acetabular coverage may become hypertrophic to make up for undercoverage of bone. Thus, the size of the labrum, particularly the acetabular coverage, depends on the patient-specific situation. Myers et al[20] evaluated hip joint stability in fresh-frozen cadavers, testing them at various flexion angles in the intact state and then again after sectioning; they later repaired the acetabular labrum and iliofemoral ligament in a randomized order. They concluded that the iliofemoral ligament had a significant role in limiting external rotation and anterior translation of the femur, while the labrum provided a secondary stabilizing role during these motions. Furthermore, Ferguson et al[6] examined the sealing function of the labrum using finite element analysis. They reported that when a compressive load of 1200 N was applied across the hip joint model, the labrum could trap a layer of pressurized fluid between the femur and acetabulum, thereby preventing contact between the articulating surfaces. Thus, the size of the labrum is an important factor when considering biomechanics and joint stability.

3D MERGE MRI is a noninvasive technique that does not require arthrography; as such, it allows construction of a wideband high-resolution image that is less affected by artifacts. Desirable contrast and high signal intensity can be obtained using multiple echoes. In addition, radial sequence imaging can be used to visualize the entire circumference of the acetabular labrum. Radial reconstruction images are useful for diagnosis of labral tears[23]; indeed, the utility of radial sequence 3D MERGE MRI for diagnosing labral tear has been reported.[13] In the current study, we demonstrated excellent intra- and interobserver reproducibility of the measured labral size on radial image

MERGE MRI scans. Reliable measurement of the acetabular labrum makes it possible to obtain patient-specific data in each case.

One of the strengths of our study is that the acetabular labrum was reconstructed using the patient-specific size of the labrum obtained from 3D MERGE MRI measurements. In CT-based dynamic simulation analysis, it is technologically difficult to reflect the effect of soft tissue, such as the labrum. Tannast et al[26] used 3D software to identify the impingement point in patients with FAI and compared the simulations with intraoperatively defined locations of the labrum and cartilage damage. They observed that actual joint damage was found more commonly during surgery than in the computer simulation of impingement. They reported that the reliability and reproducibility of cartilage grading, and of labrum lesions and their extension, were not investigated specifically because their computer simulation did not consider soft tissue and because the actual impingement point included the adjacent chondrolabral structures. In addition, they also mentioned that motion proceeds to a small extent because of the deformable properties of the cartilage and the labrum, leading to greater damage to the involved structures. Charbonnier et al[4] reported an interesting study investigating impingement on the basis of MRI findings. They evaluated the motion of the hip joints of ballet dancers using an optical tracking system (Vicon MX 13i, Oxford Metrics PLC); the resulting computed motions were then applied to patient-specific 3D hip joint models based on MRI findings. They showed that the computed impingement zones were located mainly in the superior or posterosuperior quadrant of the acetabulum for almost all movements; these locations were relevant with respect to the radiologically diagnosed damaged zones in the labrum. In the current study, we measured the labral size on 3D MERGE MRI scans and then incorporated the data into a CT-based model created using Zed Hip. While the size of the labrum on MRI scans could be reflected in the impingement simulation, it was impossible to reflect biological characteristics, including the elasticity of the labrum. Nevertheless, we evaluated 3D dynamic simulations in FAI and BDDH cases using patient-specific CT-based bone models reflecting the labral size measured on 3D MERGE MRI scans.

In our dynamic simulation, the acetabular labrum clearly affected the ROM at the hip joint. In BDDH cases in particular, the discrepancy between the bony impingement and labral interference was significant and large because of the markedly hypertrophic labrum. In theory, because of the shallow acetabular roof, the ROM up to the point of bony impingement on dynamic simulation should be large enough without considering the labrum. However, the actual ROM at the maximum flexion–internal rotation position that will cause pain in patients with hip dysplasia with labral tear is commonly poor in the clinical setting.[25] This discrepancy could be due to several factors, one being the labral interference. In fact, the dynamic impingement test is usually evaluated during arthroscopic surgery.[15] Dynamic impingement is confirmed by visible labral interference on arthroscopy before bony impingement occurs; thus, the real situation may be similar to that observed in our computer simulation based on a reconstructed labral model. If the labral position can be identified more accurately, we can predict the effect of dynamic motion on the injured labrum. Although the clinical significance is uncertain at this point in our study, this is an initial trial to examine what happens to the labrum during hip motion.

This study has several limitations. First, we measured the size of the acetabular labrum using radial sequence MRI with a clockface description; however, the virtual labrum was reconstructed on horizontal CT images. Therefore, it is impossible to achieve perfect concordance between each section. As noted in this section, it is difficult to reflect biological structure, such as the elasticity of the labrum, using Zed Hip. In our computer analysis, labral interference was only recognized as bone-to-bone impingement, whereas actual labral interference should be considered as some kind of flexible interference between bone and labrum. Another limitation is evaluation bias because of the retrospective nature of the study. Also, the number of hip joints included was relatively small, although excellent interobserver and intraobserver agreement were achieved. Finally, the study had no negative control group, which is important with respect to patient spectrum and selection bias.

CONCLUSION

As the labrum was significantly more hypertrophic in BDDH than in FAI, the interference between the labrum and bone at the maximum internal rotation angle was significantly larger in BDDH than in FAI when evaluated using the virtual labral model. The effect of the labrum should be considered in computer simulation analysis, particularly in BDDH. Future computer simulation studies should assess the clinical significance of labral interference during hip motion in both FAI and BDDH.

REFERENCES

1. Ansede G, English B, Healy JC. Groin pain: clinical assessment and the role of MR imaging. *Semin Musculoskelet Radiol*. 2011;15(1):3-13.
2. Beck M, Kalhor M, Leunig M, Ganz R. Hip morphology influences the pattern of damage to the acetabular cartilage: femoroacetabular impingement as a cause of early osteoarthritis of the hip. *J Bone Joint Surg Br*. 2005;87(7):1012-1018.
3. Byrd JWT, Jones KS. Hip arthroscopy in the presence of dysplasia. *Arthroscopy*. 2003;19(10):1055-1060.
4. Charbonnier C, Kolo FC, Duthon VB, et al. Assessment of congruence and impingement of the hip joint in professional ballet dancers: a motion capture study. *Am J Sports Med*. 2011;39(3):557-566.
5. Domayer SE, Ziebarth K, Chan J, Bixby S, Mamisch TC, Kim YJ. Femoroacetabular cam-type impingement: DIAGNOSTIC sensitivity and specificity of radiographic views compared to radial MRI. *Eur J Radiol*. 2011;80(3):805-810.
6. Ferguson SJ, Bryant JT, Ganz R, Ito K. The acetabular labrum seal: a poroelastic finite element model. *Clin Biomech (Bristol, Avon)*. 2000; 15(6):463-468.
7. Fujii M, Nakashima Y, Sato T, Akiyama M, Iwamoto Y. Pelvic deformity influences acetabular version and coverage in hip dysplasia. *Clin Orthop Relat Res*. 2011;469(6):1735-1742.
8. Fujii M, Nakashima Y, Yamamoto T, et al. Acetabular retroversion in developmental dysplasia of the hip. *J Bone Joint Surg Am*. 2010;92(4): 895-903.

9. Ganz R, Parvizi J, Beck M, Leunig M, Nötzli H, Siebenrock KA. Femoroacetabular impingement: a cause for osteoarthritis of the hip. *Clin Orthop Relat Res*. 2003;417:112-120.
10. Garabekyan T, Ashwell Z, Chadayammuri V, et al. Lateral acetabular coverage predicts the size of the hip labrum. *Am J Sports Med*. 2016; 44(6):1582-1589.
11. Hatta T, Yamamoto N, Sano H, et al. Three-dimensional morphometric analysis of the coracohumeral distance using magnetic resonance imaging. *Orthop Rev (Pavia)*. 2017;9(1):6999.
12. Henak CR, Abraham CL, Anderson AE, et al. Patient-specific analysis of cartilage and labrum mechanics in human hips with acetabular dysplasia. *Osteoarthritis Cartilage*. 2014;22(2):210-217.
13. Higashihira S, Kobayashi N, Oishi T, et al. Comparison between 3-dimensional multiple-echo recombined gradient echo magnetic resonance imaging and arthroscopic findings for the evaluation of acetabular labrum tear. *Arthroscopy*. 2019;35(10):2857-2865.
14. Ida T, Nakamura Y, Hagio T, Naito M. Prevalence and characteristics of cam-type femoroacetabular deformity in 100 hips with symptomatic acetabular dysplasia: a case control study. *J Orthop Surg Res*. 2014;9:93.
15. Kobayashi N, Inaba Y, Kubota S, et al. Computer-assisted hip arthroscopic surgery for femoroacetabular impingement. *Arthrosc Tech*. 2018;7(4):e397-e403.
16. Kobayashi N, Inaba Y, Kubota S, et al. The distribution of impingement region in cam-type femoroacetabular impingement and borderline dysplasia of the hip with or without cam deformity: a computer simulation study. *Arthroscopy*. 2017;33(2):329-334.
17. Koo TK, Li MY. A guideline of selecting and reporting intraclass correlation coefficients for reliability research. *J Chiropr Med*. 2016;15(2): 155-163.
18. Kutty S, Schneider P, Faris P, et al. Reliability and predictability of the centre-edge angle in the assessment of pincer femoroacetabular impingement. *Int Orthop*. 2012;36(3):505-510.
19. Lewis CL, Sahrmann SA. Acetabular labral tears. *Phys Ther*. 2006; 86(1):110-121.
20. Myers CA, Register BC, Lertwanich P, et al. Role of the acetabular labrum and the iliofemoral ligament in hip stability. *Am J Sports Med*. 2011;39(suppl):85S-91S.
21. Omori Y, Yamamoto N, Koishi H, et al. Measurement of the glenoid track in vivo as investigated by 3-dimensional motion analysis using open MRI. *Am J Sports Med*. 2014;42(6):1290-1295.
22. Pierannunzii L. Femoroacetabular impingement: question-driven review of hip joint pathophysiology from asymptomatic skeletal deformity to end-stage osteoarthritis. *J Orthop Traumatol*. 2019;20:32.
23. Plötz GMJ, Brossmann J, Von Knoch M, Muhle C, Heller M, Hassenpflug J. Magnetic resonance arthrography of the acetabular labrum: value of radial reconstructions. *Arch Orthop Trauma Surg*. 2001;121(8):450-457.
24. Potter HG, Nestor BJ, Sofka CM, Ho ST, Peters LE, Salvati EA. Magnetic resonance imaging after total hip arthroplasty: evaluation of periprosthetic soft tissue. *J Bone Joint Surg Am*. 2004;86(9): 1947-1954.
25. Suenaga E, Noguchi Y, Jingushi S, et al. Relationship between the maximum flexion-internal rotation test and the torn acetabular labrum of a dysplastic hip. *J Orthop Sci*. 2002;7(1):26-32.
26. Tannast M, Goricki D, Beck M, Murphy SB, Siebenrock KA. Hip damage occurs at the zone of femoroacetabular impingement. *Clin Orthop Relat Res*. 2008;466(2):273-280.
27. Yamasaki T, Yasunaga Y, Shoji T, Izumi S, Hachisuka S, Ochi M. Inclusion and exclusion criteria in the diagnosis of femoroacetabular impingement. *Arthroscopy*. 2015;31(7):1403-1410.